ELSEVIER

Catalysis Today 28 (1996) 351–362

CATALYSIS TODAY

Structure–activity relationship in Sb-V-oxide catalysts for the direct synthesis of acrylonitrile from propane

Gabriele Centi *, Paolo Mazzoli

Dip. di Chimica Industriale e dei Materiali, V. le Risorgimento 4, 40136 Bologna, Italy

Abstract

The structure/composition and catalytic behavior in propane ammoxidation to acrylonitrile of Sb-V-oxides prepared by a novel precipitation–deposition method is reported and the nature of the active components in these catalysts is discussed. Results suggest that the active phase for the selective synthesis of acrylonitrile from propane is a trirutile-like V-antimonate with Sb^{5+}-oxide supported on it. Vanadium plays a catalytic role in the selective activation of propane and reoxidation of antimony, but when present in large amounts on the surface catalyzes the unselective $NH_3 \rightarrow N_2$ conversion with a lowering in acrylonitrile selectivity. α-Sb_2O_4 is instead a side phase, with a marginal or negligible role in the catalytic behavior.

Keywords: Structure–activity relationship; Sb-V-oxide catalysts; Synthesis; Acrylonitrile from propane

1. Introduction

The development of effective catalysts for the selective functionalization of alkanes is one of the challenges in the research on mixed-oxide catalysts [1]. However, (i) the absence of specific centers on the alkane for its absorption and selective activation and (ii) the considerably higher reactivity of the possible intermediates/products makes it very difficult to find selective catalysts, especially using conversions of real interest for process development. The conversion of *n*-butane to maleic anhydride over $(VO)_2P_2O_7$ catalysts [2] is the only example of industrial use of an alkane feedstock in an oxidation process, but the ammoxidation of propane to acrylonitrile represents a second example with a significant outlook for industrial application [3,4]. Various catalysts have been proposed in patent literature for propane ammoxidation [5–7], but in several cases an initial step of gas-phase homogeneous propane to propene oxidehydrogenation occurs with a consequent difficult scale-up of the data. Sb-V-oxide catalysts, on the contrary, are able to convert selectively first propane to propene and then propene to acrylonitrile [7–11] due to the contemporaneous presence of an element active for the first step (vanadium is a key element in all catalysts active in alkane oxidehydrogenation [5]) and of a structural oxide matrix active for the second step (Sb-based catalysts with a rutile structure are well known catalysts for propene ammoxidation [12]). However, the more severe reaction conditions required for the first step of alkane activation (higher reaction temperatures, longer contact

* Corresponding author. Fax: (+39-51) 6443680, E-mail: CENTI@SCIROCCO.UNIME.IT

PII S0920-5861(96)00048-X

times) enhance the possibility of side reactions causing a significant lowering of the selectivity to acrylonitrile from propane with respect to that from propene [13]. The control of the rate of the side reaction of NH_3 unselective oxidation to N_2, in particular, is a key factor in determining the selectivity to acrylonitrile [7,8] such that the catalytic performances of Sb-V-oxide catalysts for propane ammoxidation depend critically on the preparation methodology and the reaction conditions.

Optimization of the behavior of Sb-V-oxide catalysts thus requires a thorough analysis of the relationship between structural/surface characteristics and catalytic properties. Although some general indications on this problem have already been reported in the literature [8–18], a more specific study is lacking.

The objective of the research reported here was to analyze the composition and structural characteristics of Sb-V-oxide catalysts prepared with different V:Sb ratios and correlate the observations with the catalytic behavior of the samples. Sb-V-oxide catalysts prepared by five different methods were studied, but for the sake of clarity and conciseness only data for a single, most selective, preparation method are discussed in this work. However, the results presented on the structure/activity relationship are those found also to be valid for the other preparation methods. Various characterization aspects of the samples prepared by other methods have been reported previously [15,18]. Limited attention is given in this work to the analysis of the surface characteristics of Sb-V-oxide catalysts. Sb-V-oxides before and after catalytic tests were studied by X-ray photoelectron spectroscopy in a previous work [11], and a poor correlation with the catalytic behavior due to the presence of a complex multiphasic system was observed. Catalytic tests for this study were made using a high propane concentration and having O_2 as the limiting reactant. In fact, these reaction conditions have been shown in several patents to be the more interesting for the development of the process using this kind of catalyst [5].

2. Experimental

2.1. Preparation of the catalysts

Samples were prepared by a precipitation–deposition method not previously reported in the open and patent literature. VCl_3 is dissolved in a 0.1 N aqueous HCl solution to give a dark green transparent solution (solution A). $SbCl_5$ is dissolved in a 3–5 N HCl aqueous solution to give an yellow solution (solution B). The dropwise addition of solution A to solution B leads to the formation of a white precipitate (mainly Sb-hydroxide) and a dark blue solution due to VO^{2+} ions. The latter derive from the oxidation of V^{3+} to VO^{3+} due to the two electron redox reaction of Sb^{5+} with V^{3+} and the rapid reaction of VO^{3+} with V^{3+} to form VO^{2+}. VO^{2+} is then precipitated over the Sb-hydroxide by adding dropwise a concentred aqueous solution of ammonia up to basic pH. The precipitate is filtered, washed three times with distilled water and then dried at 140°C overnight. The resulting solid is then calcined in a flow of air up to 600°C (3 h) using a constant rate of increase in temperature (50°C h^{-1}). The surface area of the samples after calcination and steady-state catalytic tests is 21, 17, 18, 10 m^2 g^{-1} for samples with an Sb:V atomic ratio of 0.8, 1.0, 2.0 and 3.0, respectively. Characterization of the samples by SEM-EDX mapping shows the absence of any inhomogeneity in the samples (V:Sb local ratio at the higher resolution was found to be equal to the global ratio determined at low magnification).

2.2. Characterization of the samples

X-ray diffraction (XRD) analysis was carried out using the powder method and a Philips PW1840 diffractometer with Cu K_α radiation. TiO_2 (anatase) added in calibrated amounts was used as an internal standard for quantitative determinations and as a reference for the evaluation of the unit cell parameters estimated on the basis of the 8 more intense reflections of the

rutile tetragonal cell. Infrared (IR) analysis was carried out with a Perkin-Elmer FT-IR 1750 instrument using the KBr disc technique and calibrated amounts of the samples. Spectra were recorded in air using a 2 cm^{-1} resolution. Scanning electron micrographs with mapping of the V and Sb distribution using electron dispersive X-ray analysis (SEM-EDX) were recorded with a JEOL 32 instrument.

Catalytic tests were carried out in a conventional plug-flow-type reactor with on-line gas-chromatographic (GC) analysis (two GCs equipped with a flame ionization and thermoconductivity detector, respectively). Ammonia conversion and HCN formation were instead detected by absorption in appropriate solutions and titration [8–11]. Tests were made using 3–4 g of sample with particle dimensions in the 0.1–0.2 mm range and diluted in a 1:5 ratio using an inert support in order to ensure an homogeneous radial and axial temperature profile. The axial temperature profile was continuously monitored by a series of thermocouples inserted into the catalytic bed. A continuous fixed-bed stainless steel reactor was used for the catalytic tests, after having checked the absence of significant mass and heat transfer limitations in the standard reaction conditions. Tests were made using the following feedstock: 7.5% propane and a O_2/C_3 and NH_3/C_3 ratio of 1.56 and 1.60, respectively. The gas-space hourly velocity (GHSV) was 2800 h^{-1}.

3. Results and discussion

3.1. Composition of Sb-V-oxide catalysts

Brief general aspects of the phase composition in Sb-V-oxide catalysts are initially discussed to provide a common background for a more clear analysis of the specific data of the preparation method used in this work.

The phase composition of Sb-V-oxide catalysts depends on four main factors: (i) method of preparation, (ii) temperature, (iii) gas phase composition during the thermal treatment, and (iv) Sb:V atomic ratio [15,18]. Various methods of preparation have been cited in the literature [18]which can be classified into two broad classes: (a) solid state reaction between the two oxides (V_2O_5 and Sb_2O_3, usually) and (b) solid state reaction between vanadium and antimony in a mixed hydroxide, where V and Sb may be present in different oxidation states depending on the preparation methodology.

Solid state reaction between vanadium and antimony occurs in the 350–500°C range [18] and usually involves a two electron redox reaction between V^{5+} and Sb^{3+} to form the $VSbO_4$ rutile phase. In the rutile phase, antimony is present as Sb^{5+} as shown by ^{121}Sb Mössbauer analysis in calcined samples with an Sb:V ratio of 1 [19], whereas based on the charge balance vanadium is formally present as V^{3+}. However, due to (i) the easy non-stoichiometry of the rutile phase [15,18–22] and (ii) the possible intergrowth of the isostructural V^{4+}-oxide, the $VSbO_4$ may be better described as a $(V^{3+}$–$V^{4+})Sb_{1-x}O_4$ mixed-valence compound [15]. When the Sb:V ratio is higher than 1.0 (stoichiometric value to form $VSbO_4$), the excess of antimony is present as α-Sb_2O_4 or β-Sb_2O_4, the latter for calcination temperatures higher than about 800°C [18]. In fact, the $\alpha \rightarrow \beta$-Sb_2O_4 transition is shifted to temperatures about 150°C lower than in pure Sb-oxide due to a catalytic effect of V on the phase transition, possibly due to partial incorporation of V into the β-Sb_2O_4 lattice [18,22–24].

Other minor phases such as V_2O_5, Sb_6O_{13} and Sb_2O_3 are sometimes detected by X-ray diffraction (XRD) analysis, depending on the preparation conditions [18], but usually these side bands are absent for calcination temperatures above about 600°C and proper preparation. According to XRD characterization, Sb-V-oxide catalysts may thus be described as mono-phasic ($VSbO_4$) or bi-phasic ($VSbO_4 + Sb_2O_4$) systems, depending on the Sb:V ratio.

Infrared spectroscopy (IR) reveals, however, that additional phases not detected by XRD are

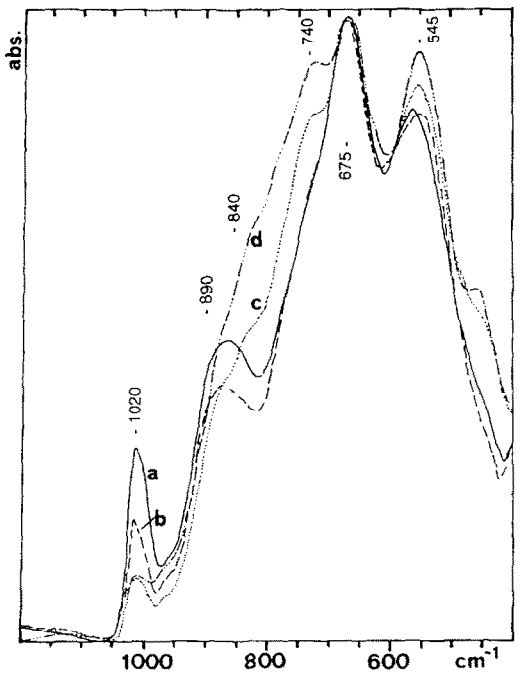

Fig. 1. Infrared spectra of calcined Sb-V-oxide samples prepared by a precipitation–deposition method: (a) Sb:V = 0.8, (b) Sb:V = 1.0, (c) Sb:V = 2.0 and (d) Sb:V = 3.0.

present in Sb-V-oxide catalysts. Reported in Fig. 1 are the IR spectra of samples with increasing Sb:V ratios in the 0.8–3.0 range and prepared by the precipitation–deposition method used in this work. For the sample with Sb:V = 0.8, clearly evident bands of V^{5+}-oxide are detected at 1020 and 840 cm^{-1} ($\nu_{V=O}$ and δ_{VOV}, respectively), together with bands due to ν_{SbO} modes of the antimonate group in the rutile structure (675 and 545 cm^{-1} [15,18,25]). The XRD pattern of the same samples shows the presence only of rutile. At the higher Sb:V ratios, XRD indicates the formation of weak reflections of α-Sb_2O_4 only for Sb:V $\geq$ 2, whereas IR spectroscopy (Fig. 1) already indicates the presence of this phase in the sample with Sb:V = 1.0 (shoulder at about 740 cm^{-1}).

Bands due to V^{5+}-oxide are still evident in the sample with Sb:V = 3.0, showing that the reaction of antimony with vanadium to form V-antimonate is not complete even for a large excess of antimony.

An evident shoulder at 890 cm^{-1} is also noted in all samples (Fig. 1). A mechanical mixture of Sb_6O_{13} and $VSbO_4$ also shows a clear shoulder at 890 cm^{-1}. This band can thus be assigned to Sb^{5+}-oxide supported over $VSbO_4$ crystallites; further aspects of this assignment are discussed later. This shoulder increases in relative intensity as the Sb:V ratio increases. The map of V and Sb distribution obtained by X-ray dispersive analysis combined with scanning electron microscopy (EDX-SEM) does not indicate local dishomogeneities in the Sb:V ratio in samples with Sb:V = 1.0 and 2.0, whereas for higher ratios Sb-oxide crystallites are detected.

In summary, data indicate that calcined Sb-V-oxide catalysts may not be considered as only monophasic $VSbO_4$ or biphasic $VSbO_4$ + Sb_2O_4 systems, but instead an overlayer of well dispersed V^{5+}- and Sb^{5+}-oxides is present over former crystallites. With increasing Sb:V ratio, there is a change in the relative amounts of these overlying, XRD amorphous phases, in addition to the change from a monophasic to biphasic system. The disappearance of V^{5+}-oxide is not complete, even for samples with a large excess of antimony.

3.2. Modification in phase composition after catalytic tests

Reported in Fig. 2 are the IR spectra of the same samples of Fig. 1, but after they had been used to ammoxidize propane to acrylonitrile at 480°C (temperature of the maximum in acrylonitrile selectivity) up to reaching a steady-state catalytic behavior after about 5–6 h of time on stream. In comparison with fresh samples (Fig. 1), a drastic decrease in the relative intensity of the band assigned to V^{5+}-oxide is observed in the samples after catalytic tests (Fig. 2). The band, however, does not completely disappear, but the maximum shifts from 1020 cm^{-1} to about 980 cm^{-1}. The shift is analogous to that observed in V_2O_5-TiO_2 catalysts [26] upon thermal spreading of vanadium and formation of a

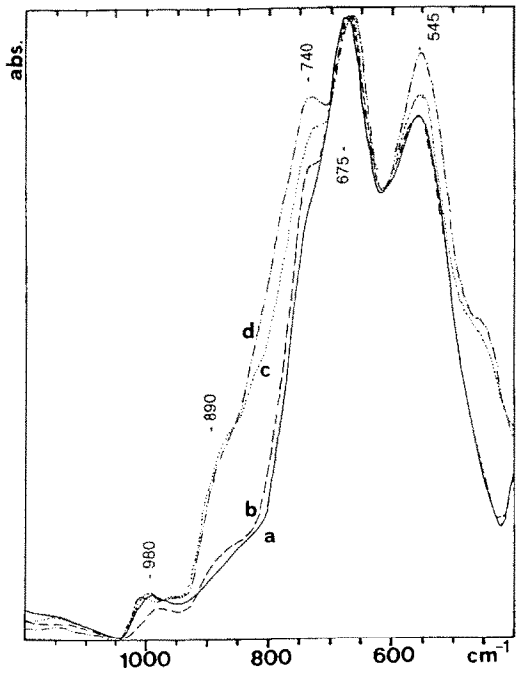

Fig. 2. Infrared spectra of the same samples of Fig. 1, but after catalytic tests in propane ammoxidation at 480°C for 6 h.

monolayer of hydrated V^{5+}-oxide. It may be concluded that during catalytic reaction most of the V^{5+}-oxide reduces, especially in samples with low Sb:V ratio, but a thin film or patches of V^{5+}-oxide over V-antimonate crystallites is still present after catalytic tests.

Vanadium, reduced during the catalytic reaction, reasonably forms V^{4+} ions, because (i) a rapid redox reaction between V^{3+} and V^{5+} to form 2 V^{4+} was observed [15] and (ii) V^{3+} is easily reoxidized in the presence of gaseous oxygen. However, V^{4+} ions formed during the catalytic reaction may (a) remain spread over V-antimonate or Sb_2O_4 crystallites or (b) react with them to form a V_2O_4-$VSbO_4$ solid solution. Furthermore, in some cases the reaction between reduced vanadium and antimony oxides [27]:

$$Sb_2O_4 + V_2O_3 + Sb_2O_3 \rightarrow 2VOSb_2O_4$$

was observed [15,18], even though this phase was always detected in small amounts. In order to distinguish between these possibilities in the samples of Figs. 1 and 2, various structural aspects of the catalysts (a) before and (b) after catalytic tests and (c) after catalytic tests and consecutive oxygen treatment at 500°C for 3 h were analyzed. Results for the sample with Sb:V = 2.0 are summarized in Table 1. After catalytic tests, reoxidation of the sample does not lead to complete restoration of the initial amount of V^{5+}, even when calcination is prolonged for longer times. This suggests that the reduction of V^{5+} during catalytic tests leads also to a change in its dispersion/interaction with V-antimonate or antimony-oxide crystallites. On the other hand, the amount of crystalline $VSbO_4$ does not change significantly before and after catalytic tests (Table 1), nor was the formation of a side phase such as $VOSb_2O_4$ detected. The only modification observed regards the cell volume of the rutile phase which

Table 1
Comparison of the structural properties of Sb-V-oxide (Sb:V = 2.0, preparation by precipitation–deposition) (a) before and (b) after catalytic tests in propane ammoxidation and (c) after catalytic tests and consecutive oxygen treatment at 500°C for 3 h

Type of treatment	V^{5+} [a]	$VSbO_4$ [b]	$VSbO_4$, unit cell volume [c] (Å^3)	$VOSb_2O_4$ [d]
Calcined sample	0.20	1.00	65.08	no
After catalytic tests	0.05	1.03	65.49	no
After catalytic tests and consecutive oxidation	0.09	0.98	65.46	no

[a] Relative intensity of the $\nu_{V^{5+}=O}$ IR band with respect to the IR band at 675 cm^{-1} of V-antimonate.
[b] Amount of crystalline $VSbO_4$ (relative to amount of $VSbO_4$ in the sample after calcination) determined by XRD analysis using TiO_2 (anatase) as the internal standard and comparing the area of the (110) reflection of $VSbO_4$ with that of the (101) reflection of TiO_2.
[c] Unit cell volume of the $VSbO_4$ phase (tetragonal) determined by fitting on the 8 most intense lines of the rutile structure.
[d] Presence of the side phase $VOSb_2O_4$ determined by XRD and IR analyses; in the latter case the presence of this phase is indicated by a sharp band centered at 980 cm^{-1} due to $\nu_{V^{4+}=O}$.

expands after catalytic tests with a reduction in the c/a ratio. The cell volume for rutile V_2O_4 is 58.97 [28] and thus a decrease in the cell volume is expected in the case of the formation of a solid solution between V_2O_4 and $VSbO_4$ rutile phases, whereas the c/a ratio may changes in a more complex way [29]. As discussed in more detail later, the expansion of cell volume is instead consistent with a change from a rutile to a trirutile structure as a consequence of the dissolution of Sb^{5+} into rutile and cation ordering to form the trirutile superstructure [30,31]. The results thus suggest that during catalytic reaction V^{5+}-oxide reduces to V^{4+}-oxide, but the dissolution of this into V-antimonate to form a solid solution is limited as well as the reaction of reduced vanadium with antimony oxide to form V-antimonate or side phases (Table 1). Tentatively, the lower rate of reoxidation of reduced vanadium-oxide after catalytic tests may be interpreted as due to the formation of a surface intergrowth of V^{4+}-oxide patches over the V-antimonate phase or of a stabilization of the latter on the reoxidation of supported V^{4+} ions. Sb^{5+}-oxide instead reacts with the rutile V-antimonate phase leading to a structural reorganization and formation of trirutile-like cation ordering. In agreement, it may be noted from the comparison of Figs. 1 and 2 that the shoulder at 890 cm^{-1} assigned to surface Sb^{5+}-oxide decreases to a more limited extent as compared to the change observed for V^{5+}-oxide. A fast reduction to Sb_2O_4 is instead observed using Sb_6O_{13} only as catalysts. The data of Figs. 1 and 2, on the contrary, indicate that the amount of Sb_2O_4 phase in the catalysts (monitored from the IR band at 740 cm^{-1}) before and after catalytic tests does not change significantly.

3.3. Nature of rutile V-antimonate phase

In iron-antimonate, catalyst active for propylene ammoxidation and isostructural with Sb-V-oxide [12], an expansion of the rutile cell volume has been observed with increasing Sb:Fe ratio above 1.0 [12,32]. The effect was interpreted as due to the formation of a non-stoichiometric rutile phase by excess antimony. Berry et al. [30,31] instead indicated by electron diffrac-

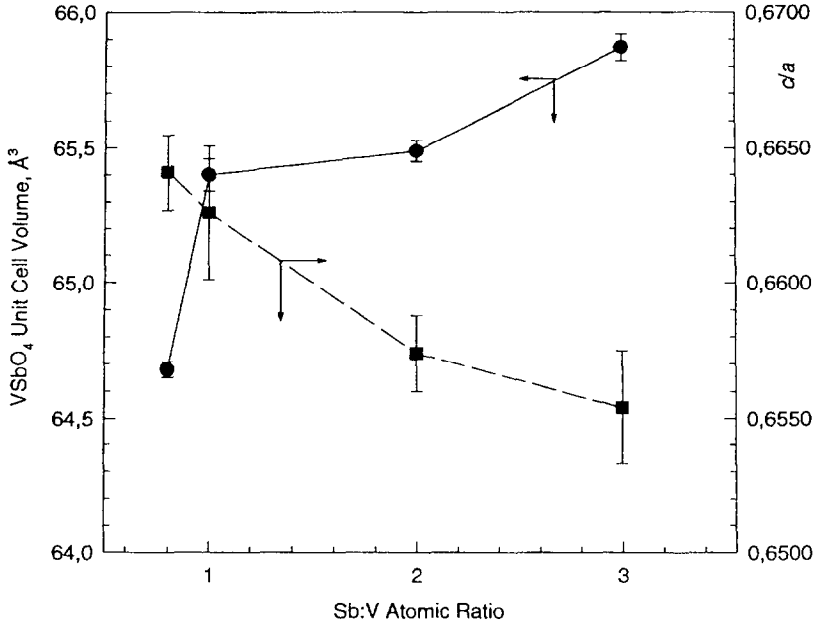

Fig. 3. Cell volume and c/a ratio in the rutile V-antimonate unit cell as a function of the Sb:V ratio in samples after catalytic tests.

tion studies the presence of cation ordering in iron-antimonate with the formation of a trirutile-like superstructure. Estimated diffraction maxima in the trirutile structure were analogous to those of the monorutile structure with the absence of detectable superlattice reflections [30]. Therefore, even in diffractograms obtained by neutron diffraction on iron-antimonate [33], the distinction between mono- and tri-rutile cation ordering is difficult. On the other hand, structural/electronic considerations on the rutile cell [28,29,34,35] suggest that an expansion of the rutile cell volume together with a contraction in the c/a cell dimensions may be expected in the change from mono- to tri-rutile like cation ordering due to the incorporation of Sb^{5+} into antimonate.

Due to the structural analogies between Fe-Sb-oxides and Sb-V-oxides, an analogous effect of cation ordering in the latter catalysts may be expected. Summarized in Fig. 3 are data regarding the structural analysis of the cell parameters of the tetragonal rutile cell in Sb-V-oxide catalysts with an increasing Sb:V ratio; the data refer to the samples after catalytic tests (the same samples of Fig. 2). With increasing Sb:V ratio, a change in the rutile cell parameters consistent with that expected for an increasing contribution of trirutile-like cation ordering was found. Although not conclusive, the data suggest that increasing the Sb:V ratio not only (a) decreases the amount of V^{5+}-oxide overlayer, (b) increases the amount of amorphous Sb^{5+}-oxide overlayer and (c) increases the presence of crystalline α-Sb_2O_4, but also (d) changes the structural characteristics of the rutile phase with an increased contribution of long-range trirutile-like cation ordering.

3.4. Catalytic behavior in propane ammoxidation

As indicated in the introduction, catalytic tests were carried out using a high propane concentration and oxygen as the limiting reagent, because in both the open and patent literature

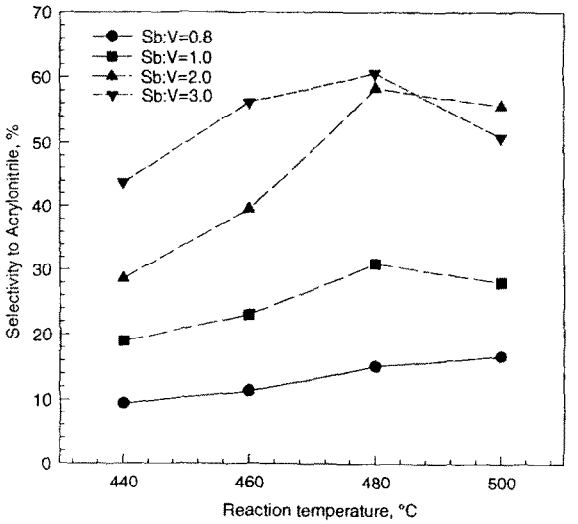

Fig. 4. Selectivity to acrylonitrile as a function of the reaction temperature and Sb:V atomic ratio. Experimental conditions as indicated in the experimental section.

these reaction conditions have been indicated as preferable for process development using this kind of catalyst [7,17]. It may be remarked, however, that a dependence between optimal catalyst composition and feedstock composition was observed, although selected reaction conditions lead to a higher selectivity to propene and acrylonitrile. Care must be taken, therefore, when extrapolating conclusions derived from this work in discussing the behavior of catalysts using different feedstocks.

Reported in Fig. 4 is the selectivity to acrylonitrile (moles of acrylonitrile formed with respect to moles propane converted) as a function of the reaction temperature for samples with increasing Sb:V ratio. The data refer to the steady-state behavior observed after about 5–6 h of time on stream. During the activation time an increase in the selectivity to acrylonitrile with a parallel decrease in the selectivity to propylene and in the rate of side oxidation of ammonia to N_2 was observed [16]. The selectivity to acrylonitrile passes through a maximum for a temperature of about 480°C for samples having a Sb:V ratio ≥ 1.0. Throughout the range of temperatures, the Sb:V ratio significantly affects the selectivity to acrylonitrile.

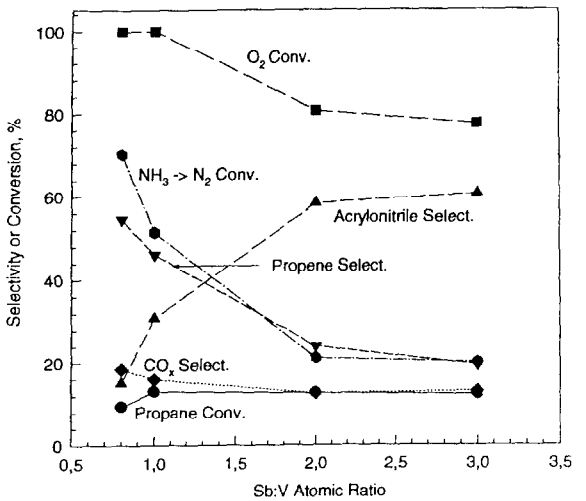

Fig. 5. Catalytic behavior of samples at 480°C as a function of the Sb:V atomic ratio. Experimental conditions as indicated in the experimental section.

Summarized in Fig. 5 is the effect of the Sb:V ratio on the catalytic behavior using as a reference for temperature that of the maximum in acrylonitrile selectivity (480°C). As the Sb:V ratio increases from 0.8 to 3.0 the selectivity to acrylonitrile increases from about 15% to above 60% with a parallel decrease in the selectivity to propene from about 55% to 20%. The selectivity to carbon oxides decreases only slightly from about 20% to 15%, whereas the conversion of propane is nearly constant. A drastic decrease is instead noted in the side reaction of unselective conversion of ammonia to N_2 and in parallel to the total conversion of ammonia; the trend with the Sb:V atomic ratio parallels closely the decrease in propene selectivity. Due to the decrease in the rate of this side reaction, the conversion of oxygen (limiting reactant) also decreases from 100% (Sb:V $\leq$ 1.0) to 80% (Sb:V = 3.0).

3.5. Relationship between catalytic behavior and catalyst structure / composition

The data of Fig. 5 show that with increasing Sb:V ratio (i) the rate of the side reaction of ammonia conversion to N_2 decreases considerably and (ii) the sum of selectivities to propene and to acrylonitrile remain nearly constant, but their relative ratio changes. It was also previously observed that with increasing Sb:V ratio various aspects of the phase composition in Sb-V-oxide catalysts are modified: (a) the amount of supported V^{5+}- and Sb^{5+}-oxides decreases and (b) the amount of α-Sb_2O_4 increases. Furthermore, the structural characteristics of the rutile phase also change due to the incorporation of Sb^{5+} and formation of long-range order (trirutile-like cation ordering). The role of supported V^{5+}-oxide in catalyzing the selective oxidation of ammonia to N_2 is known (for example, in V-oxide supported over TiO_2 [36]). It is thus reasonable initially to attribute the decrease in the rate of the side reaction $NH_3 \rightarrow N_2$ to the lowering in the amount of unreacted surface V^{5+}-oxide with increasing Sb:V ratio. However, due to the change of other sample characteristics at the same time, an unequivocal relationship cannot be established. In order to obtain a better understanding of this behavior, changes in the phase composition in Sb-V-oxide samples as a function of the Sb:V ratio were estimated by deconvolution of their IR spectra. Although when a complex mixture is present, care always must be taken in estimating phase composition by spectral deconvolution, the procedure may give a useful rough estimation of the presence of possible relationships between phase composition and catalytic behavior.

Reported in Fig. 6 is an example of the spectral deconvolution made for the Sb:V = 2.0 sample after catalytic tests. In this deconvolution the spectra of the individual crystalline, pure phases (V_2O_5, α-Sb_2O_4, Sb_6O_{13} and $VSbO_4$) are used for the simulation. Good qualitative overall fitting is found with, however, a clear lack of fitting in the 950–800 cm^{-1} region. Crystalline antimonate or antimony oxides do not have bands in this region and, on the other hand, the absorption in this region in clearly present in samples before calcination and increases for higher Sb:V ratios (see Fig. 1).

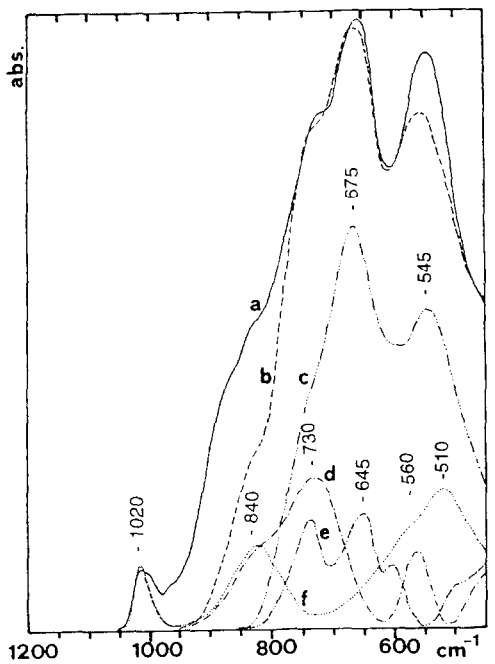

Fig. 6. Simulation (spectrum b) of the IR spectrum of an Sb:V = 2.0 sample after catalytic tests (spectrum a) on the basis of the sum of IR spectra of pure crystalline phases: (c) $VSbO_4$, (d) Sb_6O_{13}, (e) α-Sb_2O_4 and (f) V_2O_5.

An assignment of the absorption in the 950–800 cm^{-1} region to reduced V-oxide species is thus not consistent with the data. However, in a sample prepared by gently mixing Sb^{5+}-hydroxide with pure $VSbO_4$ followed by calcination at 500°C (1 h) the presence of a broad shoulder in the 950–800 cm^{-1} region was observed [18] which clearly does not originate from the simple overlap of the spectra of Sb_6O_{13} and $VSbO_4$ (see Fig. 6). This suggests that the absorption band centred at around 900 cm^{-1} may be tentatively assigned to surface Sb^{5+} ions dispersed over the V-antimonate. It should be noted that a shoulder centred at 890 cm^{-1} is present in the IR spectrum of Sb_6O_{13} or $Sb_2O_5 \cdot nH_2O$ [37]. The relative intensity of this band may be enhanced by the structural modification of Sb^{5+}-oxide deriving from its spreading over the V-antimonate phase.

The change in the relative amount of the various species in Sb-V-oxides may thus be tentatively estimated as follows: (i) for V^{5+}-oxide, by using the intensity of the band near 1000 cm^{-1}, (ii) for α-Sb_2O_4, by determining the intensity of the band at 740 cm^{-1} after subtracting the contribution of the $VSbO_4$ phase by deconvoluting the spectra and (iii) for Sb^{5+}-oxide, by using the band at 890 cm^{-1} after subtracting the contribution of $VSbO_4$ and V_2O_5 phases by deconvoluting the spectra. The relative amounts of these phases are expressed as % after normalization of the spectra to the same intensity of the band at 680 cm^{-1}. For V^{5+}-oxide the amount is relative to that of V^{5+}-oxide in the calcined Sb:V = 0.8 sample, whereas for α-Sb_2O_4 and Sb^{5+}-oxide the percentage is relative to the amount of these phases in the Sb:V = 3.0 sample after catalytic tests.

Reported in Fig. 7a is the conversion of ammonia to N_2 plotted as a function of the relative amount of V^{5+}-oxide in the sample before and after catalytic tests. As discussed above, it is reasonable to assume that the rate of ammonia side conversion to N_2 is inversely related to the amount of surface ammonia species available for the step involving the transformation of the propene intermediate to acrylonitrile and thus to the acrylonitrile to propene ratio (see Fig. 5). A good correlation between the side conversion of ammonia and the relative amount of V^{5+} is observed (Fig. 7a), but only in the calcined sample. The relationship is negligible in the catalysts after the catalytic tests (Fig. 7a). Catalytic data, however, refer to the behavior observed in steady-state conditions and thus in theory the relationship should be observed with the phase composition in the catalysts after catalytic tests.

In the previous section it was reported that V^{5+}-oxide reduces to V^{4+}-oxide during the catalytic reaction, but with a limited dissolution of V^{4+} inside the rutile phase, at least within the time on stream studied. V^{4+} was suggested to be present mainly as small domains of V^{4+}-oxide on the surface intergrown with the V-antimonate rutile phase. Reasonably, this phase although stabilized with respect to redox reoxidation to V^{5+}-oxide, may also be active in ammo-

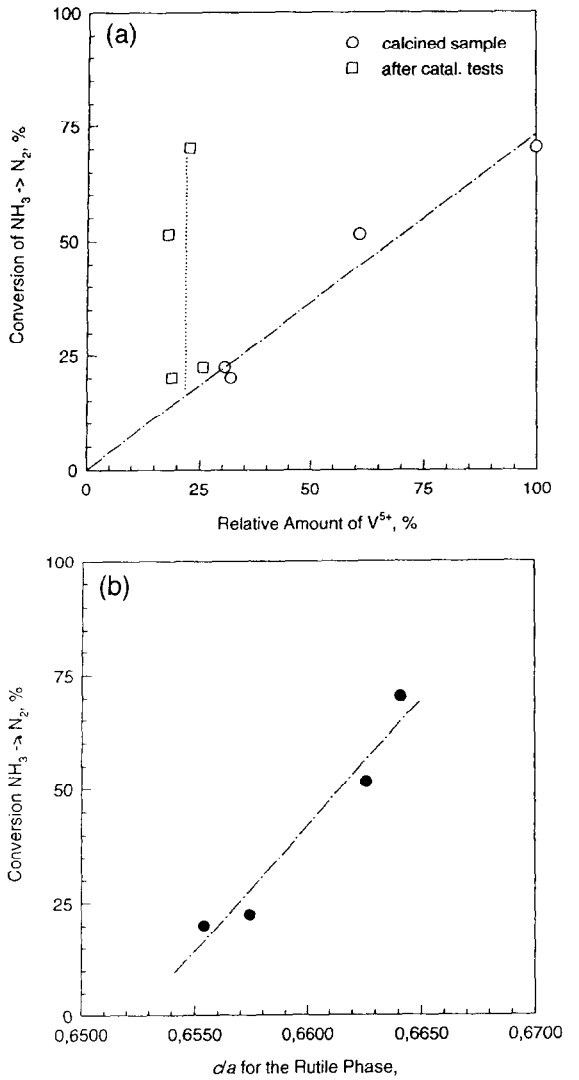

Fig. 7. (a) Correlation between relative amounts of V^{5+}-oxide before and after catalytic tests (see text) and conversion $NH_3 \rightarrow N_2$ at 480°C in samples with different Sb:V ratios. (b) Correlation between c/a ratio in the unit cell of the rutile phase (samples after catalytic tests) and conversion $NH_3 \rightarrow N_2$ at 480°C in samples with different Sb:V ratios.

nia side conversion to N_2. The amount of V^{5+}-oxide in the calcined sample is thus an index of the total amount of vanadium present on the surface of the V-antimonate crystallites that has not reacted with antimony to form a Sb-V mixed oxide. The data reported in Fig. 7a therefore suggest that the rate of the side conversion of ammonia to N_2 should be correlated to the total amount of supported vanadium-oxide in Sb-V-oxide samples after catalytic tests (amount proportional to V^{5+} in calcined sample) more than directly to the amount of residual V^{5+}-oxide after catalytic tests.

Parallel to the change in the amount of unreacted vanadium-oxide with increasing the Sb:V ratio, a change in the structural characteristics of the V-antimonate phase was also observed. Reported in Fig. 7b is the relationship between the change in these characteristics using the c/a ratio of the rutile cell after catalytic tests as the index and the conversion of $NH_3 \rightarrow N_2$. As discussed above, the decrease in the c/a ratio in the rutile cell may be associated with long-range cation ordering from the mono- to tri-rutile unit cell due to the reaction of excess surface Sb^{5+} with rutile V-antimonate. This also implies a surface reconstruction of the V-antimonate phase with a possible change in its reactivity towards the unselective conversion of ammonia to N_2. The data reported in Fig. 7b show that a rough correlation exists between long-range trirutile-like cation ordering and decrease in the conversion of $NH_3 \rightarrow N_2$. This suggests that the decrease in the side conversion of ammonia with a consequent increase in the acrylonitrile/propene ratio with increasing Sb:V atomic ratio may be attributed not only to the decrease in the total amount of vanadium not stabilized by formation of a Sb-V mixed-oxide, but also to the change in the surface reactivity properties of the rutile phase due to its long-range cation ordering.

Reported in Fig. 8 is the correlation between selectivity to acrylonitrile and the amount of supported Sb^{5+}-oxide and of α-Sb_2O_4 estimated as described above. The results suggest a roughly linear relationship between selectivity to acrylonitrile and amount of supported Sb^{5+}-oxide, whereas correlation with the amount of α-Sb_2O_4 may be considered negligible. This suggests that the latter phase may be considered as a side phase with limited, or negligible functionality in the mechanism of propane ammoxidation to acrylonitrile. Supported Sb^{5+}-oxide

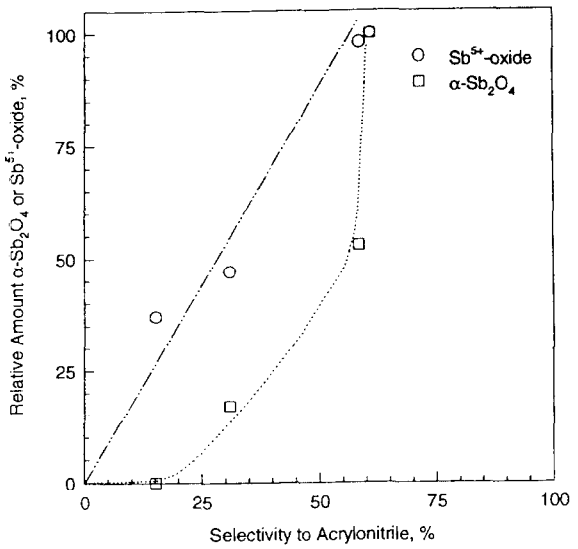

Fig. 8. Correlation between selectivity to acrylonitrile at 480°C in samples with different Sb:V ratios and amounts of Sb^{5+}-oxide and α-Sb_2O_4 phases in samples after catalytic tests (see text).

plays instead a catalytic role in determining the selectivity to acrylonitrile. This confirms the data of Fig. 7b suggesting that the surface modification of the rutile V-antimonate phase due to the reaction with supported Sb^{5+}-oxide is a key aspect of the surface reactivity of Sb-V-oxides and determines the ratio of the rates of ammonia side conversion to N_2 and of ammonia used for propene conversion to acrylonitrile.

The analysis of the structure/composition and activity relationship thus suggests that the active phase for the selective synthesis of acrylonitrile from propane is a trirutile-like V-antimonate with Sb^{5+}-oxide supported on it. Vanadium probably plays a catalytic role in the selective activation of propane in agreement with the selective formation of propene for Sb:V $\leq$ 1.0. However, when present in large amounts on the surface vanadium catalyzes the unselective $NH_3 \rightarrow N_2$ conversion with a lowering in acrylonitrile selectivity. In addition, vanadium is probably necessary to facilitate reoxidation of antimony [11,17]. α-Sb_2O_4 is instead a side phase, with a probably marginal or negligible role on the catalytic behavior.

References

[1] G. Centi, in R.W. Joyner and R.A. van Santen (Editors), Elementary Reaction Steps in Heterogeneous Catalysis, NATO Symposium Series, Kluwer Academic, Dordrecht, The Netherlands, 1993, p. 93.
[2] G. Centi, Catal. Today, 16 (1993) 5.
[3] Chem. Eng., 8 (1990) September 13.
[4] A. Pavone and R.H. Schwaar, PEP Rev., 2/4 (1989) 88.
[5] F. Trifirò and F. Cavani, Catal. Stud., (1994) 419350.
[6] Y. Moro-oka and W. Ueda, in Catalysis, Vol. 11, The Royal Society of Chemistry, Cambridge, UK, 1994, p. 223.
[7] G. Centi, R.K. Grasselli and F. Trifirò, Catal. Today, 13 (1992) 661.
[8] G. Centi, R.K. Grasselli, E. Patanè and F. Trifirò, in G. Centi and F. Trifirò (Editors), New Developments in Selective Oxidation, Elsevier, Amsterdam, 1990, p. 515.
[9] G. Centi, D. Pesheva and F. Trifirò, Appl. Catal., 33 (1987) 343.
[10] R. Catani, G. Centi, F. Trifirò and R.K. Grasselli, Ind. Eng. Chem. Res., 31 (1992) 107.
[11] A. Andersson, S.L.T. Andersson, G. Centi, R.K. Grasselli, M. Sanati and F. Trifirò, Appl. Catal. A, 113 (1994) 43.
[12] G. Centi and F. Trifirò, Catal. Rev., Sci. Eng., 28 (1986) 165.
[13] R. Nilsson, T. Lindblad and A. Andersson, J. Catal., 148 (1994) 501.
[14] R. Nilsson, T. Lindblad, A. Andersson, C. Song and S. Hansen, in V. Cortes Corberan and S. Vic Bellon (Editors), New Developments in Selective Oxidation II, Elsevier, Amsterdam, 1994, p. 281.
[15] G. Centi, E. Foresti and F. Guarneri, in V. Cortes Corberan and S. Vic Bellon (Editors), New Developments in Selective Oxidation II, Elsevier, Amsterdam, 1994, p. 281.
[16] G. Centi and S. Perathoner, Appl. Catal. A, 124 (1995) 317.
[17] A. Andersson, S.L.T. Andersson, G. Centi, R.K. Grasselli, M. Sanati and F. Trifirò, in L. Guczi et al. (Editors), New Frontiers in Catalysis, Elsevier, Amsterdam, 1993, p. 691.
[18] G. Centi, S. Perathoner, in G. Poncelet et al. (Editors), Preparation of Catalysts VI, Elsevier, Amsterdam, 1995, p. 59.
[19] T. Birchall and A.E. Sleight, Inorg. Chem., 15 (1976) 868.
[20] F.J. Berry, M.E. Brett and W.R. Patterson, J. Chem. Soc., Dalton Trans., (1983) 9.
[21] F.J. Berry, M.E. Brett and W.R. Patterson, J. Chem. Soc., Dalton Trans., (1983) 13.
[22] R.G. Teller, M.R. Antonio, J.F. Brazdil and R.K. Grasselli, J. Solid State Chem., 64 (1986) 249.
[23] F.J. Berry, M.E. Brett, R.A. Marbrow, W.R. Patterson, J. Chem. Soc., Dalton Trans., (1984) 985.
[24] F.J. Berry and M.E. Brett, J. Catal., 88 (1984) 232.
[25] C. Rocchiccioli-Deltcheff, T. Dupuis, R. Frank, M. Harmelin and C. Wadier, C.R. Acad. Sci. Paris B, 270 (1970) 541.
[26] G. Centi, D. Pinelli, F. Trifirò, D. Ghoussoub, M. Guelton and L. Gengembre, J. Catal., 130 (1991) 238.
[27] B. Darriet, J. Bovin and J. Galy, J. Solid State Chem., 19 (1976) 205.
[28] D.B. Rogers, R.D. Shannon, A.W. Sleight and J.L. Gillson, Inorg. Chem., 8 (1969) 841.

[29] H. Baur and A.A. Khan, Acta Crystallogr., B27 (1971) 2133.
[30] F.J. Berry, J.G. Holden and M.H. Loretto, J. Chem. Soc., Faraday Trans. 1, 83 (1987) 615.
[31] F.J. Berry, J.G. Holden and M.H. Loretto, Solid State Commun., 59 (1986) 397.
[32] M. Carbucicchio, G. Centi and F. Trifirò, J. Catal., 91 (1985) 85.
[33] R.G. Teller, J.F. Brazdil, R.K. Grasselli and, W. Yelon, J. Chem. Soc., Faraday Trans. 1, 41 (1985) 1693.
[34] P.I. Sorantin and K. Schwarz, Inorg. Chem., 31 (1992) 567.
[35] J.K. Burdett, Inorg. Chem., 24 (1985) 2244.
[36] F. Cavani and F. Trifirò, Catal. Today, 4 (1989) 253.
[37] C.A. Cody, L. DiCarlo and R.K. Darlington, Inorg. Chem., 18 (1979) 1572.